Specific Absorption Rate and Temperature Increases in the Head of a Cellular-Phone User

Paolo Bernardi, *Fellow, IEEE*, Marta Cavagnaro, Stefano Pisa, *Member, IEEE*, and Emanuele Piuzzi

***Abstract*—In this paper, a complete electromagnetic and thermal analysis has been performed considering the head of a subject exposed to various kinds of cellular phones available on the market, and focusing the attention on important organs like the eye lens and brain. Attention has first been posed on a particular phone model, and a comparison between the absorbed power distribution and steady-state temperature increases has been carried out. The influence of different antennas (dipole, monopole, whip, and planar inverted F antenna) on the power absorption and on the consequent tissue heating has then been analyzed. The obtained results show, for a radiated power of 600 mW, maximum SAR values, averaged over 1 g, from 2.2 to 3.7 W/kg depending on the considered phone. The maximum temperature increases are obtained in the ear and vary from 0.22 °C to 0.43 °C, while the maximum temperature increases in the brain lie from 0.08 °C to 0.19 °C. These steady-state temperature increases are obtained after about 50 min of exposure, with a time constant of approximately 6 min. Finally, the results evidence a maximum temperature increase in the external part of the brain from 0.10 °C to 0.16 °C for every 1 W/kg of SAR, averaged over 1 g of brain tissue.**

***Index Terms*—Biological effects of electromagnetic radiation, dosimetry, electromagnetic heating, FDTD methods, land mobile radio cellular systems, temperature.**

I. Introduction

THE ever-rising diffusion of cellular mobile radio systems has determined an increased concern for possible users' health effects due to the field emitted by the handheld terminals. In fact, when a cellular phone is working, the transmitting antenna is placed very close to the user's head where a substantial part of the radiated power is absorbed.

Up to now, the most recognized RF exposure standards adopt the SAR, averaged over the whole body ($\mathrm{SAR_{WB}}$), as the basic parameter to establish the safety of an exposure [1]–[4]. The value of 4 W/kg is accepted worldwide as the threshold for the induction of biological thermal effects. In the setting up of RF standards, a safety factor of 50 for general public (or uncontrolled) exposure has been introduced, giving rise to a basic limit on $\mathrm{SAR_{WB}}$ equal to 0.08 W/kg.

When the power absorption takes place in a confined body region, as in the case of the head exposed to a cellular phone, even if the $\mathrm{SAR_{WB}}$ is well below the basic limit, the local SAR can assume rather high values. For this reason, limits on local SAR averaged over tissue masses of 1 or 10 g have been introduced in the standards. These local limits have been chosen, increasing the basic limit on $\mathrm{SAR_{WB}}$ of a factor from 20 to 25, giving rise to the well-known values of 1.6 W/kg over 1 g [1], [2] or 2 W/kg over 10 g [3], [4].

However, to consider local or average SAR as the basic parameter in assessing possible thermal biological effects does not seem completely satisfactory. In fact, the tissue heating is strongly influenced not only by the power dissipated in the local tissue volume, but also by the way in which absorption is distributed in the surrounding area, by the thermal characteristics of the considered and neighboring tissues, and finally, by the heat exchanges with the external environment [5], [6]. Consequently, the correlation between local SAR values and temperature increases and between SAR and thermal distributions is not straightforward. Therefore, a thermal analysis seems to be necessary, in addition to SAR analysis, to assess the safety of an exposure.

Many studies have been performed in the past for calculating the power absorbed in a human body exposed to the electromagnetic (EM) field emitted by radio-communication equipment (see [7] and [8]), but only a few papers [9]–[13] have dealt with the evaluation of the corresponding temperature increases. In particular, in [12], starting from SAR values measured in a phantom head exposed to handheld mobile phones, steady-state temperature rises were calculated, using a simplified thermal model for the brain, while in [13], the attention was focused on a human head under plane-wave exposure.

Studying the bioelectromagnetic interaction from a thermal point-of-view, it is interesting to compare the obtained temperature increases with the thresholds for the induction of thermal damages.

The threshold temperature increase for neuron damage is about 4.5 °C (for more than 30 min) [14]. Experiments performed on the eye have evidenced a threshold increase of 3 °C–5 °C in the lens for the induction of the cataract [15], [16]. The temperature increase necessary to induce thermal damage in the skin is at least 10 °C [17], [18]. Finally, experiments performed on animals have evidenced various physiological effects when the body core temperature rises more than 1 °C–2 °C [4].

In this work, we have evaluated the power absorption and the corresponding temperature increases induced in an anatomical heterogeneous model of the human head exposed to the field emitted by a portable phone operating around 900 MHz. In particular, we have compared phones equipped with different kinds of antennas [half-wavelength dipole, quarter-wavelength monopole, whip, and planar inverted F antenna (PIFA)].

Manuscript received January 20, 1999.

The authors are with the Department of Electronic Engineering, University "La Sapienza" of Rome, 00184 Rome, Italy (e-mail: bernardi@die.ing.uniroma1.it).

Publisher Item Identifier S 0018-9480(00)05470-3.

II. Methods and Models

The SAR spatial distribution in a human-head model has been computed by using the finite-difference time-domain (FDTD) numerical technique. The FDTD has been applied in its classical formulation [19], [20] with second-order absorbing boundary conditions [21]. Starting from the evaluated SAR distribution, the thermal response as a function of time, until the steady state is reached, has been calculated through an explicit finite-difference formulation of the bioheat equation.

The power radiated in free space from the various types of telephones has been computed both on the basis of the feed point impedance and Poynting's vector flow obtaining a good agreement between the two. The generator impedance has been assumed matched to the antenna free-space radiation impedance, with a voltage amplitude suitable to obtain a radiated power of 600 mW in free space. It should be noted that when analyzing the coupling between a phone and human head, the radiated power decreases due to the change of the antenna radiation impedance [22].

The SAR values averaged over 1 g (SAR_1) and over 10 g (SAR_{10}) have been computed considering tissue masses in the shape of a cube with a volume of approximately 1 and 10 cm^3, respectively. Only cubes weighting at least 0.8 g for SAR_1 and 8 g for SAR_{10} have been examined.

A. Head and Hand Model

The head model considered in this study has been obtained from the one realized at the Radiology Department, Yale University, New Haven, CT [23]. This model, developed from magnetic resonance imaging (MRI) scans of a human head, had a spatial resolution of 1.1 × 1.1 × 1.4 mm from the top of the head to the ear-lobe level and a resolution of 4 × 4 × 4 mm in the remaining part of the head.

For obtaining a good accuracy of the EM solution with the FDTD method at the frequencies of interest, a cell dimension of 2 mm is sufficient. Therefore, the original model has been resampled to obtain a final resolution of 2 × 2 × 2 mm. Sixteen different types of tissues and organs have been evidenced, and particular attention has been devoted to the modeling of the ear that has been compressed to a thickness of 6 mm in order to simulate its morphology during a phone call.

The tissue parameters used in the FDTD simulations are given in Table I. The reported values are the results of recent measurements performed on freshly excised animals [24] and refer to a frequency of 900 MHz.

In some simulations, the hand grasping the phone has been considered. The hand tissue has been assigned electric properties equal to two-thirds of those used for the muscle. The hand is wrapped around the case on three sides, leaving free the side facing the head.

B. Phone Models

Four cellular-phone models have been considered. The first two are the half-wavelength dipole and the quarter-wavelength monopole on a conducting box, which are canonical phone models usually found in literature [25]–[30]. The last two are realistic models, one equipped with the whip antenna, and the other with the side-mounted PIFA.

TABLE I
Mass Density and Dielectric Parameters of the Head Tissues at 900 MHz

	ρ [kg/m^3]	ε_r	σ [S/m]
Skin	1010	41.4	0.87
Muscle	1040	55.0	0.94
Bone	1810	21.0	0.32
Blood	1060	61.4	1.54
Fat	920	11.3	0.11
Cartilage	1100	40.8	0.81
Grey matter	1040	54.7	1.19
White matter	1040	35.7	0.61
Humor	1010	74.1	1.97
Lens	1100	51.3	0.89
Sclera/Cornea	1170	52.1	1.22
Cerebellum	1040	49.6	1.03
Hypophysis	1040	49.6	1.03
CSF	1010	74.0	2.12
Parotid	1040	49.6	1.03
Tongue	1040	57.0	0.80

The monopole and dipole antennas have been modeled within the FDTD code as infinitely thin conductors by zeroing the field component along the wire axis.

The whip antenna is constituted of a five-eighths wavelength monopole with a coil (electrical length $\lambda/8$) at its basis fed by the inner conductor of a coaxial cable protruding outside the box [31]. In the practical manufacture of the whip antenna, the monopole is realized by using a wire wound to form a thin helix to reduce the physical length of the antenna. In the FDTD program, the monopole has been modeled by using a stack of lumped inductances, the basis coil has been realized with a staircase approximation [22], [32], and the feeding conductor has been modeled with a stack of conductor cells [see Fig. 1(a)].

Both the monopole and whip antennas are mounted on the top of a conducting box (1.4 × 4.8 × 12 cm), which is covered with a dielectric insulator (4-mm thick, $\varepsilon_r = 2$). In particular, the antenna is located on the top surface, 1 cm far from the posterior short side, and centered with respect to it [see Fig. 1(a) for the whip].

The side-mounted PIFA [33] is a planar antenna constituted of a microstrip patch (electrical length $\lambda/4$) short circuited at one end. Two PIFA's are mounted on the lateral sides of a conducting box (1.4 × 5.2 × 15 cm) [see Fig. 1(b)] in order to obtain spatial diversity and to gain an improvement in the received signal when the phone operates in a multipath environment. However, only one antenna is used for the transmission mode. The whole structure is enclosed in a plastic case (4-mm thick, $\varepsilon_r = 2$). The radiation impedance of this antenna is matched to the generator internal impedance by properly positioning the feed point along the microstrip patch (for the considered geometry, 8 mm from the short). The patch has been modeled in the FDTD code as a flat conductor by zeroing the tangential electric-field components over its surface.

A vertical and a tilted position have been considered for each phone. The tilting has been chosen to bring the bottom part of the phone case in front of the mouth to simulate the realistic use position. In the FDTD code this has been obtained leaving

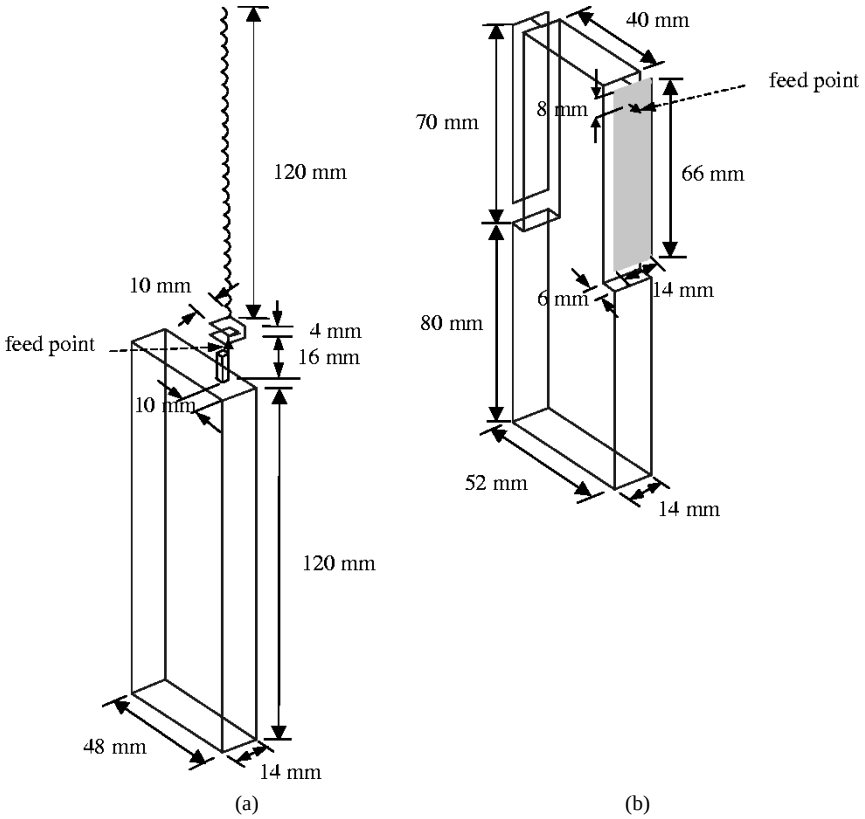

Fig. 1. Geometries and dimensions of the metallic parts of the phones. (a) Phone equipped with the whip antenna. (b) Phone equipped with the side-mounted PIFA.

the phone in the vertical position and rotating the head in the forward direction by 60°. The rotated head model has been obtained assigning to each cell of the final domain $C_F(i, j, k)$, the tissue filling the cell of the initial domain $C_I(i', j', k')$, where the center of the cell $C_F(i, j, k)$ falls after a backward 60° rotation is applied to it. This procedure altered the number of cells for each tissue less than 1%. Fig. 2 shows the obtained phone positioning with respect to the head for the handset equipped with the monopole antenna.

C. Thermal Model

The temperature distribution $T = T(\boldsymbol{r}, t)$ inside the head model has been obtained by using the bioheat equation

$$K \cdot \nabla^2 T + A_0 + Q_v - B \cdot (T - T_b) = C \cdot \rho \cdot \frac{\partial T}{\partial t} \quad \left[\mathrm{W/m^3}\right] \tag{1}$$

where K is the thermal conductivity $[\mathrm{J/(s \cdot m \cdot ^\circ C)}]$, A_0 and Q_v are volumetric heat sources $[\mathrm{J/(s \cdot m^3)}]$ due to metabolic processes and microwave power deposition, respectively, B is a parameter proportional to the blood perfusion $[\mathrm{J/(s \cdot m^3 \cdot ^\circ C)}]$, T_b is the blood temperature, and, finally, C$[\mathrm{J/(kg \cdot ^\circ C)}]$ and ρ $[\mathrm{kg/m^3}]$ are the tissue specific heat and density, respectively.

At the skin–air interface, the continuity of the perpendicular heat flow has been imposed (convective boundary condition). The heat exchanged through the neck with the remaining part of the body has been approximated by means of a further convective boundary condition. The thermoregulation mechanisms have been neglected because of the slight temperature rises induced.

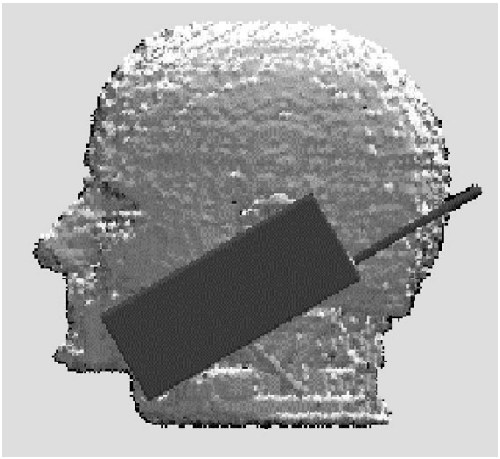

Fig. 2. Three-dimensional visualization of the tilted phone positioning with respect to the head model.

The bioheat equation and the convective boundary conditions have been solved by using the explicit finite-difference formulation presented in [5]. In particular, the temperature distribution has been evaluated with a spatial step equal to that used in FDTD calculations (2 mm). Considerations on the stability of the explicit finite-difference algorithm impose a limit on the maximum allowed time step [5], which, in this case, is about 2 s.

The thermal parameters used in (1) have been extrapolated from existing literature [14], [34]–[39] and are reported in Table II. In particular, specific heat and thermal

TABLE II
THERMAL PARAMETERS OF THE HEAD TISSUES

	C [J/(kg·°C)]	K [J/(s·m·°C)]	A_0 [J/(s·m^3)]	B [J/(s·m^3·°C)]
Skin	3500	0.42	1000	9100
Muscle	3600	0.50	690	2700
Bone	1300	0.40	0	1000
Blood	3900	0.00	0	0
Fat	2500	0.25	180	520
Cartilage	3400	0.45	1000	9100
Grey matter	3700	0.57	10000	35000
White matter	3600	0.50	10000	35000
Humor	4000	0.60	0	0
Lens	3000	0.40	0	0
Sclera/Cornea	4200	0.58	0	0
Cerebellum	3700	0.57	10000	35000
Hypophysis	3700	0.57	10000	36000
CSF	4000	0.60	0	0
Parotid	3700	0.57	7000	25000
Tongue	3300	0.42	3700	13000

conductivity values were directly available for almost all the considered tissues [34]–[36]. The missing values have been calculated starting from the percentage water content (W) of the tissue and by using the following equations reported in [34]: $C = 1670 + 25.1 \cdot \mathrm{W}$ [J/(kg ·° C)], $K = 0.0502 + 0.00577 \cdot \mathrm{W}$ [J/(s · m ·° C)]. All blood perfusion values were obtained from [14], [34], [37]–[39]. Only a few data exist on metabolic heat generation and, therefore, the missing values have been assumed proportional to the blood perfusion, as suggested in [38].

The most interesting feature to be noted in Table II is that the normal blood perfusion in the brain tissues is about ten times higher than in the other head tissues. This large blood perfusion compensates for the heat production caused by the high basal metabolic rate, maintaining a physiological temperature of about 37.5 °C in the inner brain region.

III. RESULTS AND DISCUSSION

This section is divided in two subsections. In the first, the results obtained for a particular phone model are presented in order to analyze and compare the SAR values and distribution with the corresponding temperature increases (ΔT). In the second, a comparison among the results obtained when considering different phone models is made.

A. Comparison Between SAR Distribution and Temperature Increases

The exposure of the head to a phone equipped with a whip antenna has been chosen as a reference situation. The phone is placed in the vertical position and its case is kept in direct contact with the ear. This gives rise to a distance of about 1.2 cm between the antenna feed point and the external part of the ear. The free space radiated power is 600 mW.

The results obtained are shown in the first row of Table III (as concerns SAR values) and of Table IV (ΔT values). When the head is present, the radiated power decreases to 567 mW and more than 50% of this power (313 mW) is absorbed in the head ($\mathrm{P_{abs}}$). The maximum $\mathrm{SAR_1}$ ($\mathrm{SAR_{1MAX}}$) and $\mathrm{SAR_{10}}$ ($\mathrm{SAR_{10MAX}}$) values are 2.30 and 1.14 W/kg, respectively. The maximum SAR in the brain, as averaged over 1 g ($\mathrm{SAR_{1MAXbrain}}$), is 0.93 W/kg, and finally, a maximum 1 g averaged SAR of 0.033 W/kg is obtained in the eye ($\mathrm{SAR_{1MAXeye}}$).

For the considered phone, the $\mathrm{SAR_{1MAX}}$ and $\mathrm{SAR_{1MAXbrain}}$ values are very close to those obtained in [26], [40] in similar exposure conditions. Lower values were found in [22] with a

TABLE III
TOTAL POWER ABSORBED IN THE HEAD ($\mathrm{P_{abs}}$), MAXIMUM SAR AS AVERAGED OVER 1g ($\mathrm{SAR_{1MAX}}$) AND 10g ($\mathrm{SAR_{10MAX}}$) OF TISSUE IN THE HEAD, AND MAXIMUM SAR AS AVERAGED OVER 1g OF BRAIN ($\mathrm{SAR_{1MAXbrain}}$) OR EYE ($\mathrm{SAR_{1MAXeye}}$). PHONE POSITIONS: VERTICAL (V) AND TILTED (T). POWER RADIATED IN FREE SPACE: 600 mW. FREQUENCY: 900 MHz

Phone model		P_{abs} [mW]	SAR_{1MAX} [W/kg]	SAR_{10MAX} [W/kg]	$SAR_{1MAXbrain}$ [W/kg]	$SAR_{1MAXeye}$ [W/kg]
WHIP	V	313	2.30	1.14	0.93	0.033
	T	272	2.31	1.25	0.66	0.059
MONOPOLE	V	365	2.17	1.29	1.21	0.022
	T	323	2.40	1.29	0.73	0.077
DIPOLE	V	388	2.74	1.93	1.85	0.022
	T	323	2.83	1.08	0.81	0.015
PIFA (Side mounted-frontal patch feeded)	V	428	3.72	1.88	1.22	0.071
	T	402	3.40	1.99	1.28	0.165

TABLE IV
STEADY-STATE TEMPERATURE RISE. MAXIMUM IN THE WHOLE HEAD (ΔT_{MAX}), IN THE BRAIN ($\Delta T_{\mathrm{MAXbrain}}$), AND IN THE LENS ($\Delta T_{\mathrm{MAXlens}}$). PHONE POSITIONS: VERTICAL (V) AND TILTED (T). POWER RADIATED IN FREE SPACE: 600 mW. FREQUENCY: 900 MHz

Phone model		ΔT_{MAX} [°C]	$\Delta T_{MAXbrain}$ [°C]	$\Delta T_{MAXlens}$ [°C]
WHIP	V	0.23	0.12	0.005
	T	0.25	0.08	0.008
MONOPOLE	V	0.22	0.13	0.003
	T	0.23	0.09	0.010
DIPOLE	V	0.33	0.19	0.003
	T	0.29	0.13	0.002
PIFA (Side mounted-frontal patch feeded)	V	0.43	0.14	0.011
	T	0.39	0.16	0.022

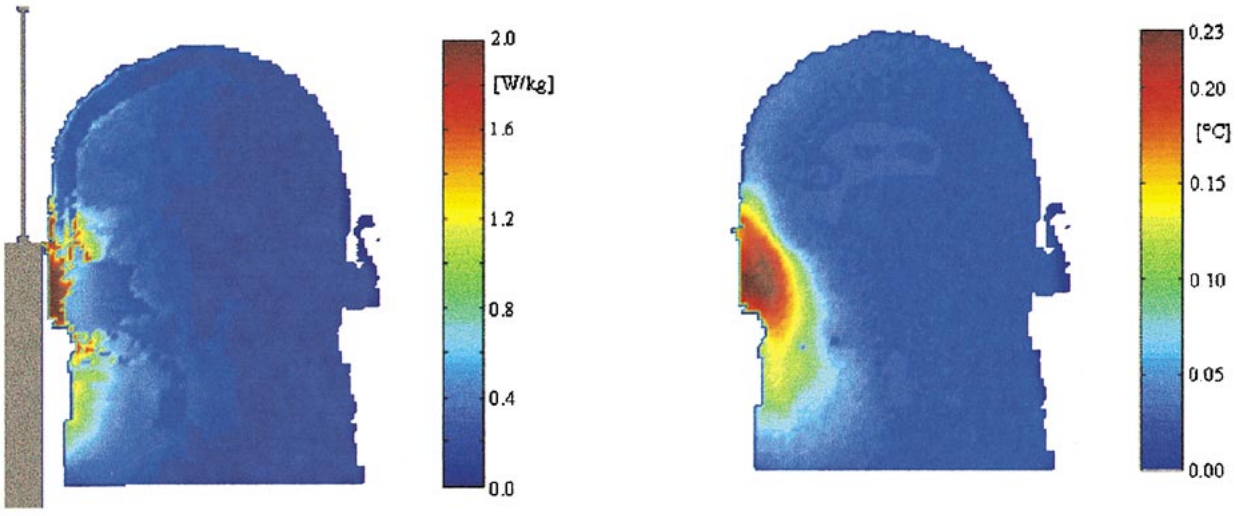

(a) (b)

Fig. 3. Frontal section of the head in which the maximum local SAR occurs for a whip phone in the vertical position. (a) SAR distribution. (b) Temperature increase distribution. Power radiated in free space: 600 mW. Frequency: 900 MHz.

different head model and with the antenna placed at a higher distance from the head. Higher values can also be found in the literature [27], [41]. The observed variability is essentially due to differences in phone geometry and position and in the used head model.

Fig. 3(a) shows the SAR distribution evaluated on the vertical section of the head in which the maximum SAR occurs. It can be noted that the highest SAR values are obtained in the central region of the ear that is in direct contact with the upper part of the phone case. From the figure, it appears that a certain amount of power absorption also takes place in the head region placed in front of the whip antenna, and in the lower part of the head (jaw, neck, and parotid gland) close to the radio case, which is part of the radiating structure.

With reference to the thermal problem, first of all, the initial temperature distribution has been evaluated solving the bioheat equation in the nonirradiated head by using the K, A_0, and B values given in Table II. The obtained distribution compares well with the physiological one [14]. After that, the temperature evolution has been evaluated taking into account the power absorption due to the field radiated by the phone. When the steady state is reached, the temperature rise (ΔT) is computed. Following this procedure, the maximum temperature rise (ΔT_{MAX}) is obtained in the ear region and is equal to 0.23 °C. A temperature rise of 0.12 °C is present in the external part of the brain close to the phone ($\Delta T_{\mathrm{MAXbrain}}$). Finally, a negligible temperature variation is observed in the eye lens ($\Delta T_{\mathrm{MAXlens}} = 0.005$ °C).

Considering the results for $\mathrm{SAR}_{1\mathrm{MAXbrain}}$ and $\Delta T_{\mathrm{MAXbrain}}$ we note that a temperature rise of 0.12 °C was induced by a local dissipation of 0.93 W/kg. This corresponds to a normalized heating factor ($\Delta T/\mathrm{SAR}_1$) of about 0.13 °C/(W/kg). In the same exposure condition, the normalized heating factor in the inner brain is 0.03 °C/(W/kg), which is more than four times lower. This different behavior is due to the fact that the maximum SAR and temperature increase in the brain are induced in the external part and not in the inner one. Consequently, since the external brain region is partly bounded by low blood perfusion and low thermal conductivity tissues (bone and fat), the cooling mechanism is less effective.

The previous considerations clearly indicate that the presence of heterogeneous tissues greatly influences the temperature increases in the brain region, and that temperature increases are not directly proportional to the local SAR values, thus confirming the importance of using a complete thermal model.

Fig. 3(b) shows the heating distribution in the same section as Fig. 3(a). From Fig. 3(b), it appears that the region where the maximum temperature increase takes place is located in the lower part of the ear.

The comparison between Fig. 3(a) and (b) shows that SAR and ΔT distributions are rather different. Due to the thermal conduction mechanism, the thermal profile penetrates to a great extent in the ear region, while the high blood perfusion present in the brain, bringing away a great amount of heat, limits the temperature rise in the upper part of the head.

The above reported thermal results refer to steady-state conditions, reached after about 50 min of exposure (however, 90% of the final ΔT is reached after about 15 min). It should be noted that a phone call usually lasts a few minutes, hence, the steady-state temperature rise is rarely reached. It is, therefore, interesting to consider the time evolution of the temperature in some significant points. Fig. 4(a) shows, for different call durations, the temperature increase in the point inside the ear where ΔT_{MAX} occurs. In Fig. 4(b), the corresponding evolution is reported for the $\Delta T_{\mathrm{MAXbrain}}$ point. In particular, exposures lasting 1, 3, 6, and 15 min are shown in the figures.

The rising part of the curves in Fig. 4(a) and (b) can be approximated with a single exponential expression of the kind $\Delta T_{\mathrm{MAX}} \cdot [1 - \exp(-t/\tau)]$. The evaluation of the time constant is straightforward and a τ value of about 6 min has been obtained for both curves.

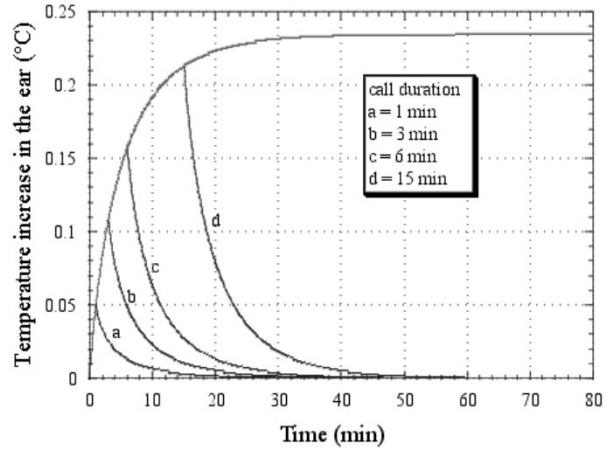

(a)

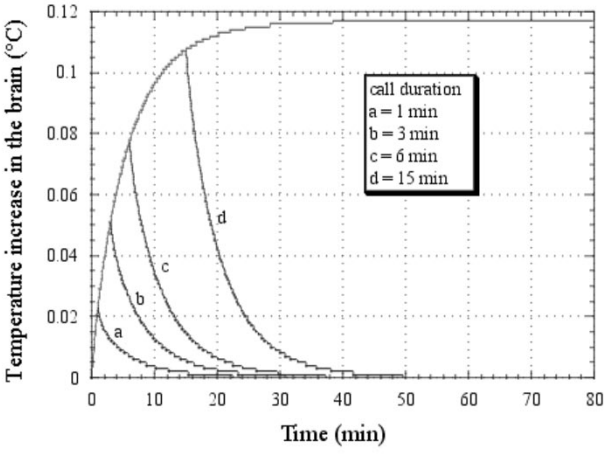

(b)

Fig. 4. Time evolution of the temperature increase for exposures lasting 1, 3, 6, and 15 min at the points where the maximum local ΔT occurs. (a) Inside the ear. (b) In the brain.

It must be observed that the above-described temperature rises are due to the power deposition induced by the field radiated by the cellular phone. Anyhow, in practical situations, two more causes for temperature increase could be present. The first is the contact between the phone case and the ear that alters thermal exchange between the skin layers and the air, causing temperature rises in the tissues around the ear. The second is the heating up of the phone itself, due to the power dissipated in the circuitry and, in particular, in the power amplifier; this heating is transmitted to the head tissues via thermal conduction. The influence of these two causes has been investigated by using the explicit finite-difference formulation of the bioheat equation. In particular, the investigation has been performed neglecting the SAR induced inside the head and considering both the contact between the phone and ear and the dissipation in the power amplifier (simulated adding a power deposition of 600 mW inside the upper part of the phone, corresponding to a 50% efficiency). Under these conditions, and after 15 min, a temperature increase of about 1 °C is obtained in the ear, while the temperature increase in the brain region closest to the ear remains below 0.04 °C. In conclusion, in the realistic use conditions, the heating of the ear seems to be mainly due to the phone contact and phone self-heating, while the SAR due to the field radiated by the phone plays an important role in the external brain heating.

B. Comparison Between Various Phone Models

Four different phone models have been analyzed (see Section II-B). All the phones radiate a power of 600 mW in free space. During the simulated phone exposure, the whip, monopole, and PIFA cases are maintained in contact with the ear. As concerns the dipole, its feed point has been placed at the same location as for the monopole and whip. For each of the considered phones, two positions [vertical (V) and tilted (T)] have been considered.

The obtained results in terms of total absorbed power and SAR values are shown in Table III.

For all the considered phones, the radiated power when the head is present is close to the available one, and half or more of this power is absorbed inside the head (see Table III, first column). As already evidenced in [22] and [42], SAR values in a given point inside the head are mainly influenced by the amplitude of the current along the antenna at the same height, and by the distance between the antenna and the point under examination.

The results for the whip phone in the vertical position have been presented and analyzed in the previous paragraph. For this phone, the tilting determines a reduction of about 13% in the absorbed power. This is due to the increase of the distance between the upper part of the antenna and head. This shift in the antenna position is also responsible for the reduction of $\mathrm{SAR_{1MAXbrain}}$. On the contrary, $\mathrm{SAR_{1MAX}}$ and $\mathrm{SAR_{10MAX}}$ values are almost the same or slightly increased and the $\mathrm{SAR_{1MAXeye}}$ value is almost doubled due to the radio case approaching the eye. Previous works by different authors [27], [33] showed a decrease in the $\mathrm{SAR_{1MAX}}$ and $\mathrm{SAR_{10MAX}}$ values for the tilted model. Our results are justified by the fact that, for the particular positioning of the phone (in close contact with the ear), the peak SAR values are obtained in correspondence of the upper part of the phone case whose distance from the head is almost unaffected by the phone tilting.

The monopole on the box gives results similar to those obtained with the phone equipped with the whip antenna with differences within 15%. Only $\mathrm{SAR_{1MAXbrain}}$ shows a 30% increase for the vertical monopole with respect to the whip phone in the same position. This result is explained by looking at the current distribution along the two antennas. In fact, at the level where $\mathrm{SAR_{1MAXbrain}}$ occurs, higher current values are present in the monopole with respect to the whip antenna. The results obtained for the monopole on the box suggest that this simplified phone model can be used for simulating real phones equipped with pull-out antennas only if an high accuracy is not required; otherwise, more precise antenna models are necessary.

The vertical dipole gives rise to $\mathrm{SAR_{1MAX}}$ and $\mathrm{SAR_{10MAX}}$ values 21% and 33% higher with respect to the monopole, with only a 6% increase in the total absorbed power. In fact, with this phone model, the power absorption is more confined with respect to the other phone models and, hence, higher local

SAR values are obtained. This is evidenced also by the 45% increase in $SAR_{1MAXbrain}$ with respect to the monopole. The tilting determines variations similar to those observed for the other phones. Only SAR_{10MAX} has a different behavior due to the increased distance between the upper antenna branch and the part of the head where SAR_{10MAX} is found. As already evidenced by other authors [26], [27], the dipole generally gives rise to an overestimation of actual SAR levels induced by phones equipped with pull-out antennas.

The phone equipped with the PIFA gives rise to the highest P_{abs} and SAR values. These values have been obtained by feeding the frontal patch antenna, which is very close to the ear and, therefore, strongly coupled with the head. This results in a strong and focalized exposure in the ear and cheek regions where high SAR_{1MAX} (3.72 W/kg) and SAR_{10MAX} (1.88 W/kg) values are found. Lower values were found in [33], but with the telephone kept further away from the head. For this phone, $SAR_{1MAXbrain}$ is relatively low with respect to the SAR_{1MAX} value, and the tilting poorly influences the coupling between the antenna and head. SAR values about one order of magnitude lower than those reported in Table III are found feeding the back patch antenna. It must be noted that, today, manufacturers tend to mount patch antennas on the back of the telephone: this configuration has been studied in literature obtaining SAR values about three times lower than those produced by a monopole antenna [41].

The exposure conditions have been replicated by considering the presence of the hand grasping the phone. In all the situations, the hand determines a reduction of the power absorbed in the head and of SAR values. This reduction is of the order of 20%–30% for the monopole and the whip, but it reaches 40% for the PIFA, which, due to the antenna position, couples more strongly with the hand.

Table IV shows the maximum temperature increases obtained in the head, brain, and lens for the four considered phone models and the two phone positions (V, T).

For all the considered phones, ΔT_{MAX} is placed in the earlobe, while the $\Delta T_{MAXbrain}$ is placed in the external part of the brain.

The whip and monopole give rise to similar ΔT_{MAX} values, which increase about 50% when considering the dipole. The highest ΔT_{MAX} values (up to 0.43 °C) are induced with the side-mounted PIFA telephone (with frontal patch fed).

With reference to $\Delta T_{MAXbrain}$, Table IV shows that the tilting produces a decrease of about 30% in the computed values, except for the PIFA where a slight increment can be observed.

Finally, Table IV shows that the temperature increase in the lens is negligible in all the situations.

From the results in Tables III and IV, the normalized heating factor, relating ΔT_{MAX} and SAR_{1MAX} in the brain, previously computed for the whip antenna, can also be evaluated for the other phone models. The obtained values lie in the range of 0.10 °C/(W/kg)–0.16 °C/(W/kg). As already pointed out, this spreading is due to the different positions in which the maximum SAR and temperature increase occur when the exposure conditions change.

IV. Conclusions

Local SAR distributions and temperature increases have been evaluated and analyzed in an anatomical heterogeneous model of the human head exposed to the field radiated by different models of cellular phones.

With reference to SAR values, the IEEE limit (1.6 W/kg over 1 g) is exceeded in all the considered situations, while the CENELEC limit (2 W/kg over 10 g) is always respected. It must be noted that these results refer to a portable phone radiating 600 mW in free space, which is typical of analog cellular phones. The new digital generation is characterized by a lower mean radiated power (250 mW). This means that the reported results should be decreased by a factor of 2.4, giving rise to SAR_{1MAX} values below the IEEE limit for all the considered phones.

The temperature increases calculated in this study with a radiated power of 600 mW are at least 20 times lower than those indicated in the literature as thresholds for the induction of thermal damage.

It is interesting to note that, for all the considered phone models, a maximum SAR_1 value of 1.6 W/kg gives rise to a temperature increase in the brain of about 0.09 °C, which is about 50 times lower than the threshold for thermal damage, while considering the CENELEC limit of 2 W/kg averaged over 10 g, the brain heating is of about 0.2 °C.

The obtained results show that temperature increases induced by the exposure cannot simply be related to SAR values at the same location due to the highly inhomogeneous structure of the head with respect to dielectric and thermal parameters.

References

[1] *IEEE Standard for Safety Levels with Respect to Human Exposure to Radio Frequency Electromagnetic Fields, 3 kHz to 300 GHz*, IEEE Standard C95.1–1991, 1992.

[2] "Evaluating compliance with FCC guidelines for human exposure to radiofrequency electromagnetic fields," Federal Communications Commission, Washington, D.C, OET Bull. 65, Aug. 1997.

[3] *Human Exposure to Electromagnetic Fields. High frequency (10 kHz to 300 GHz)*, IEEE Prestandard ENV 50 166-2, Jan. 1995.

[4] ICNIRP Guidelines, "Guidelines for limiting exposure to time-varying electric, magnetic, and electromagnetic fields (up to 300 GHz)," *Health Phys.*, vol. 74, no. 4, pp. 494–522, 1998.

[5] P. Bernardi, M. Cavagnaro, S. Pisa, and E. Piuzzi, "SAR distribution and temperature increase in an anatomical model of the human eye exposed to the field radiated by the user antenna in a wireless LAN," *IEEE Trans. Microwave Theory Tech.*, vol. 46, pp. 2074–2082, Dec. 1998.

[6] ——, "Temperature elevation induced in the head of a cellular phone user," in *Int. Sci. Meeting Electromag. Medicine*, Chicago, IL, Nov. 1997, p. 76.

[7] C. H. Durney, "The physical interactions of radiofrequency radiation fields and biological systems," in *AGARD Lecture Series.* Neuilly Sur Seine, France: NATO AGARD, 1985, pp. 2.1–2.19.

[8] J. C. Lin and O. P. Gandhi, "Computational method for predicting field intensity," in *Handbook of Biological Effects of Electromagnetic Fields*, C. Polk and E. Postow, Eds. Boca Raton, FL: CRC Press, 1995, pp. 337–402.

[9] A. Taflove and M. E. Brodwin, "Computation of the electromagnetic fields and induced temperatures within a model of the microwave irradiated human eye," *IEEE Trans. Microwave Theory Tech.*, vol. MTT-23, pp. 888–896, Nov. 1975.

[10] R. J. Spiegel, "The thermal response of a human in the near-zone of a resonant thin-wire antenna," *IEEE Trans. Microwave Theory Tech.*, vol. MTT-30, pp. 177–184, Feb. 1982.

[11] I. Chatterjee and O. P. Gandhi, "An inhomogeneous thermal block model of man for the electromagnetic environment," *IEEE Trans. Biomed. Eng.*, vol. BME-30, pp. 707–715, Nov. 1983.
[12] V. Handerson and K. H. Joyner, "Specific absorption rate levels measured in a phantom head exposed to radio frequency transmission from analog hand-held mobile phones," *Bioelectromag.*, vol. 16, pp. 60–69, 1995.
[13] Y. Lu, J. Ying, T. Tan, and K. Arichandran, "Electromagnetic and thermal simulations of 3-D human head model under RF radiation by using the FDTD and FD approaches," *IEEE Trans. Magn.*, vol. 42, pp. 1653–1656, May 1996.
[14] A. C. Guyton, *Textbook of Medical Physiology*. Philadelphia, PA: Saunders, 1991.
[15] A. W. Guy, J. C. Lin, P. O. Kramar, and A. F. Emery, "Effect of 2450-MHz radiation on the rabbit eye," *IEEE Trans. Microwave Theory Tech.*, vol. MTT-23, pp. 492–498, June 1975.
[16] B. Appleton, S. E. Hirsch, and P. V. K. Brown, "Investigation of single-exposure microwave ocular effects at 3000 MHz," *Ann. New York Academy Sci.*, vol. 247, pp. 125–134, 1975.
[17] D. H. Sliney and B. E. Stuck, "Microwave exposure limits for the eye: Applying infrared laser threshold data," in *Radiofrequency Radiation Standards*. New York: Plenum, 1994, pp. 79–87.
[18] J. D. Hardy, H. G. Wolff, and H. Goodell, *Pain Sensations and Reactions*. Baltimore, MD: Williams & Wilkins, 1952.
[19] A. Taflove, *Computational Electrodynamics: The Finite-Difference Time-Domain Method*. Norwood, MA: Artech House, 1995.
[20] K. S. Kunz and R. J. Luebbers, *The Finite Difference Time Domain Method for Electromagnetics*. Boca Raton, FL: CRC Press, 1993.
[21] G. Mur, "Absorbing boundary conditions for the finite- difference approximation of the time-domain electromagnetic-field equations," *IEEE Trans. Electromag. Compat.*, vol. EMC-23, pp. 377–382, Apr. 1981.
[22] P. Bernardi, M. Cavagnaro, and S. Pisa, "Evaluation of the SAR distribution in the human head for cellular phones used in a partially closed environment," *IEEE Trans. Electromag. Compat.*, vol. 38, pp. 357–366, Aug. 1996.
[23] I. G. Zubal, C. R. Harrell, E. O. Smith, Z. Rattner, G. R. Gindi, and P. B. Hoffer, "Computerized three-dimensional segmented human anatomy," *Med. Phys.*, vol. 21, no. 2, pp. 299–302, 1994.
[24] S. Gabriel, R. W. Lau, and C. Gabriel, "The dielectric properties of biological tissues: III. Parametric models for the dielectric spectrum of tissues," *Phys. Med. Biol.*, vol. 41, pp. 2271–2293, 1996.
[25] J. Toftgard, S. N. Hornsleth, and J. B. Andersen, "Effects on portable antennas of the presence of a person," *IEEE Trans. Antennas Propagat.*, vol. 41, pp. 739–746, June 1993.
[26] P. J. Dimbylow and S. M. Mann, "SAR calculations in an anatomically realistic model of the head for mobile communication transceivers at 900 MHz and 1.8 GHz," *Phys. Med. Biol.*, vol. 39, pp. 1537–1553, 1994.
[27] O. P. Gandhi, G. Lazzi, and C. M. Furse, "Electromagnetic absorption in the human head and neck for mobile telephones at 835 and 1900 MHz," *IEEE Trans. Microwave Theory Tech.*, vol. 44, pp. 1884–1897, Oct. 1996.
[28] M. Okoniewski and M. A. Stuchly, "A study of the handset antenna and human body interaction," *IEEE Trans. Microwave Theory Tech.*, vol. 44, pp. 1855–1864, Oct. 1996.
[29] V. Hombach, K. Meier, M. Burkhardt, E. Kuhn, and N. Kuster, "The dependence of EM energy absorption upon human head modeling at 900 MHz," *IEEE Trans. Microwave Theory Tech.*, vol. 44, pp. 1865–1873, Oct. 1996.
[30] S. Watanabe, M. Taki, T. Nojima, and O. Fujiwara, "Characteristics of the SAR distributions in a head exposed to electromagnetic fields radiated by a hand-held portable radio," *IEEE Trans. Microwave Theory Tech.*, vol. 44, pp. 1874–1883, Oct. 1996.
[31] K. Kagoshima and T. Taga, "Land mobile antennas systems I: basic techniques and applications," in *Mobile Antenna Systems Handbook*, K. Fujimoto and J. R. James, Eds. Norwood, MA: Artech House, 1994.
[32] M. Cavagnaro and S. Pisa, "Simulation of cellular phone antennas by using inductive lumped elements in the 3D/FDTD algorithm," *Microwave Opt. Technol. Lett.*, pp. 324–327, Dec. 1996.
[33] M. A. Jensen and Y. Rahmat-Samii, "EM Interaction of handset antennas and a human in personal communications," *Proc. IEEE*, vol. 83, pp. 7–17, Jan. 1995.
[34] F. A. Duck, *Physical Properties of Tissue*. New York: Academic, 1990.
[35] J. J. W. Lagendijk, "A mathematical model to calculate temperature distributions in human and rabbit eyes during hyperthermic treatment," *Phys. Med. Biol.*, vol. 27, no. 11, pp. 1301–1311, 1982.
[36] J. A. Scott, "A finite element model of heat transport in the human eye," *Phys. Med. Biol.*, vol. 33, no. 2, pp. 227–241, 1988.
[37] L. R. Williams and R. W. Leggett, "Reference values for resting blood flow to organs of man," *Clinical Phys. Physiol. Meas.*, vol. 10, no. 3, pp. 187–217, 1989.
[38] R. G. Gordon, R. B. Roemer, and S. M. Horvath, "A mathematical model of the human temperature regulatory system—Transient cold exposure response," *IEEE Trans. Biomed. Eng.*, vol. BME-23, pp. 434–444, Nov. 1976.
[39] R. J. Dickinson, "An ultrasound system for local hypothermia using scanned focused transducers," *IEEE Trans. Biomed. Eng.*, vol. BME-31, pp. 120–125, Jan. 1984.
[40] A. D. Tinniswood, C. M. Furse, and O. P. Gandhi, "Computation of SAR distributions for two anatomically based models of the human head using CAD files of commercial telephones and the parallelized FDTD code," *IEEE Trans. Antennas Propagat.*, vol. 46, pp. 829–833, June 1998.
[41] M. G. Douglas, M. Okoniewski, and M. A. Stuchly, "A planar diversity antenna for handheld PCS devices," *IEEE Trans. Veh. Technol.*, vol. 47, pp. 747–754, Aug. 1998.
[42] Q. Balzano, O. Garay, and T. J. Manning, "Electromagnetic energy exposure of simulated users of portable cellular telephones," *IEEE Trans. Veh. Technol.*, vol. 44, pp. 390–403, Aug. 1995.

Paolo Bernardi (M'66–SM'73–F'93) was born in Civitavecchia, Italy, in 1936. He received the degree in electrical engineering and the "Libera Docenza" degree in microwaves from the University of Rome, Rome, Italy, in 1960 and 1968, respectively.

Since 1961, he has been with the Department of Electronics, University of Rome "La Sapienza," Rome, Italy, where he became a Full Professor in 1976. He was Director of the Department from 1982 to 1988. His research work has dealt with the propagation of EM waves in ferrites, microwave components, biological effects of EM waves, and EM compatibility. He has authored over 150 scientific papers and numerous invited presentations at international workshops and conferences. He is an Associate Editor for the *URSI Radio Science Bulletin*, is on the Editorial Board of the *Microwave and Optical Technology Letters*, and was the Guest Editor of Special Issues of *Alta Frequenza* (Mar. 1980) on "Nonionizing Electromagnetic Radiation," and *Wireless Networks* (Dec. 1997) on "Exposure Hazards and Health Protection in Personal Communication Services."

Dr. Bernardi is a member of the Bioelectromagnetics Society (BEMS), the European Bioelectromagnetics Association (EBEA), and a "Socio Fedele" of the Italian Electrical and Electronic Society (AEI). From 1979 to 1980, he was the chairman of the IEEE Middle and South Italy Section. He was chairman of the URSI Commission K on Electromagnetics in Biology and Medicine (1993–96), chairman of a Commission of the Italian National Research Council (CNR) working on a national project on Electromagnetic Compatibility in Electrical and Electronic Systems, vice-chairman of the European Community COST Project 244 on Biomedical Effects of Electromagnetic Radiation (1993–97), and project coordinator of the European Community CEPHOS project, which is devoted to EM dosimetry and compliance with standards of mobile cellular phones. He is an Editorial Board member for the IEEE TRANSACTIONS ON MICROWAVE THEORY AND TECHNIQUES. In 1984, he was awarded the IEEE Centennial Medal.

Marta Cavagnaro was born in Rome, Italy, in 1966. She received the Electronic Engineering degree (*cum laude*) and the Ph.D. degree from the University "La Sapienza" of Rome, Rome, Italy, in 1993 and 1997, respectively.

Her current research interests are dosimetric aspects of the interaction between EM fields and biological systems, and numerical techniques.

Dr. Cavagnaro was the recipient of a 1993 scholarship presented by the Alenia Spazio S.p.A. to study the coupling between EM fields and triaxial cables and the recipient of the 1996 URSI Young Scientist Award.

Stefano Pisa (M'91) was born in Rome, Italy, in 1957. He received the electronic engineering and Ph.D. degrees from the University "La Sapienza" of Rome, Rome, Italy, in 1985 and 1988, respectively.

He is currently with the Department of Electronic Engineering, University "La Sapienza" of Rome, as a Researcher. His research interests are in the interaction between EM fields and biological systems and in therapeutic and diagnostic applications of EM fields.

Emanuele Piuzzi was born on May 25, 1972, in Lecce, Italy. He received the Electronic Engineering degree (*cum laude*) from the University "La Sapienza" of Rome, Rome, Italy, in 1997, and is currently working toward the Ph.D. degree at the University "La Sapienza" of Rome.

He is currently studying hybrid techniques for the solution of Maxwell's equations, with particular attention to those involving FDTD. His research interests are RF dosimetry, heating induced inside human beings exposed to RF and microwave fields, and hybrid numerical techniques for EM-field computation.